The role of miR-143-3p/FNDC1 axis on the progression of non-small cell lung cancer

Zhanshu Ma, Qi Gao, Wenjing Xin, Lei Wang, Yan Chen, Chang Su, Songyan Gao, Ruiling Sun

Department of Radiotherapy, Affiliated Hospital of Chifeng University, Chifeng, China

ABSTRACT

The study aimed to explore the functional role of fibronectin type III domain containing 1 (FNDC1) in non-small cell lung cancer (NSCLC), as well as the mechanism governing its expression. The expression levels of FNDC1 and related genes in tissue and cell samples were detected by qRT-PCR. Kaplan-Meier analysis was employed to analyze the association between FNDC1 level and the overall survival of NSCLC patients. Functional experiments such as CCK-8 proliferation, colony formation, EDU staining, migration and invasion assays were conducted to investigate the functional role of FNDC1 in regulating the malignancy of NSCLC cells. Bioinformatic tools and dual-luciferase reporter assay were used to identify the miRNA regulator of FNDC1 in NSCLC cells. Our data revealed the upregulation of FNDC1 at mRNA and protein levels in NSCLC tumor tissues cancer cell lines, compared with normal counterparts. NSCLC patients with higher FNDC1 expression suffered from a poorer overall survival. FNDC1 knockdown significantly suppressed the proliferation, migration and invasion of NSCLC cells, and had an inhibitory effect on tube formation. We further demonstrated that miR-143-3p was an upstream regulator of FNDC1 and miR-143-3p expression was repressed in NSCLC samples. Similar to FNDC1 knockdown, miR-143-3p overexpression inhibited the growth, migration and invasion of NSCLC cells. FNDC1 overexpression could partially rescue the effect of miR-143-3p overexpression. FNDC1 silencing also suppressed the tumorigenesis of NSCLC cells in mouse model. In conclusion, FNDC1 promotes the malignant prototypes of NSCLC cells. miR-143-3p is a negative regulator of FNDC1 in NSCLC cells, which may serve as a promising therapeutic target in NSCLC.

Key words: FNDC1; miR-143-3p; non-small cell lung cancer (NSCLC).

Non-commercial use only

Correspondence: Ruiling Sun, Department of Radiotherapy, Affiliated Hospital of Chifeng University, No. 42 Wangfu Street, New Town, Songshan District, 024099 Chifeng City, China. Tel. +86.0476.5973012.
E-mail: gret258@163.com

Contributions: ZM, RS, mainly participated in literature search, study design, writing and critical revision; QG, WX, LW, YC, CS, SG, mainly participated in data collection, data analysis and data interpretation. All the authors read and approved the final version of the manuscript and agreed to be accountable for all aspects of the work.

Conflict of interest: the authors declare that they have no competing interests, and all authors confirm accuracy.

Ethics approval and consent to participate: the study was approved by the Ethics Committee Board of Affiliated Hospital of Chifeng University and written informed consent was obtained from each patient in accordance with institutional guidelines. All animal procedures were approved by the Animal Care and Use Ethical Committee of Affiliated Hospital of Chifeng University.

Availability of data and material: the datasets during and/or analyzed during the current study are available from the corresponding author on reasonable request.

Introduction

Lung cancer, a highly invasive and metastatic malignancy, remains as one of the leading cancer type globally.[1] Lung cancer can be categorized into non-small cell lung cancer (NSCLC) and small cell lung cancer (SCLC), with NSCLC accounting for 80% and SCLC 20% of total lung cancer cases.[2] Despite advances in diagnostic approaches such as computed tomography (CT) and the proposed usage of certain biomarkers, the incidence and mortality of lung cancer is continue rising.[3,4] This may be due to tumor heterogeneity and the difficulty in diagnosing lung cancer at early stage. Patients at early stage can be treated with optimal surgical resection, together with neoadjuvant or adjuvant therapy. Chemo- and targeted-therapies have been widely used in patients at advanced stages, such as platinum, gefitinib or bevacizumab.[5] Even though these drugs show promising clinical effect in certain patients, the 5-year overall survival of lung cancer patients remains under 20%.[6] Therefore, the investigation of molecular mechanisms underlying the malignant progression of lung cancer might contribute to the formulation of novel anti-cancer strategies.[7,8]

Fibronectin is a cell surface glycoprotein family present in extracellular matrix, which is implicated in cellular mobility and cell differentiation. Although fibronectin contributes to fibrotic pathobiology, its role in cancer biology remains controversial.[9] Fibronectin Type III Domain Containing 1 (FNDC1) is a protein-coding and disease-related gene that encodes a protein containing conserved fibronectin type III domain.[10] It is primarily located in the nuclear speckles and involved in the regulation of multiple cellular processes, such as proliferation, migration, metabolism and apoptosis.[11] In cancer biology, there is increasing evidence regarding the dysregulation of FNDC1 in tumor progression. The upregulation of intracellular FNDC1 is closely related to distal metastasis of breast cancer.[12] FNDC1 overexpression has also been related to skin tumor progression, which may be regulated by TGF-β and inflammatory cytokines.[13] FNDC1 may also serve as an oncogenic factor in prostate cancer cells, and the knockdown of FNDC1 showed an inhibitory effect on cell proliferation and migration.[14] Besides, FNDC1 is highly expressed in gastric cancer and elevated FNDC1 expression is associated with a dismal prognosis in the patients, which could be attributed to enhanced metastatic potential in gastric cancer patients.[15] Although there is abundant evidence supporting the oncogenic role FNDC1 in many cancer types, its role in NSCLC remains to be clarified. Additionally, only few studies investigated the mechanisms underlying FNDC1 upregulation in tumor cells. For example, miR-1207-3p was identified as an upstream regulator of FNDC1 in prostate cancer.[14] How FNDC1 becomes dysregulated in other cancers is largely unknown.

In this study, we aim to investigate the expression pattern of FNDC1 in NSCLC tumors, study its functional role in regulating NSCLC cell malignancy and clarify the mechanism underlying its dysregulation in NSCLC. We reported the overexpression of FNDC1 in NSCLC tumor samples and human NSCLC cell lines compared to the normal counterparts. FNDC1 knockdown suppressed the malignant phenotype of NSCLC cells, including cell growth, migration and invasion. miR-143-5p was identified as a miRNA regulator to suppress the expression of FNDC1. miR-143-5p level was reduced in tumor samples and cancerous cell lines, and its overexpression impaired the malignancy of NSCLC cells. Importantly, we showed that silencing FNDC1 could attenuate tumor growth of NSCLC cells in mouse model. Our findings established the oncogenic function of FNDC1 in NSCLC, identified miR-143-3p as the negative regulator of FNDC1, and highlighted miR-143-3p/FNDC1 axis as a promising therapeutic target in NSCLC.

Materials and Methods

Cells and cancer samples

Human NSCLC cell lines (H1975, A549, CALU6, CALU3, H1229) and the normal human bronchial epithelial cells (HBE) were purchased from ATCC. Cells were cultured in Dulbecco's modified Eagle medium (DMEM, Gibco, Thermo Fisher Scientifics, Waltham, MA, USA) containing 10% FBS, 100 U/mL penicillin and 100 μg/mL streptomycin. Tumor samples and para-cancerous pulmonary specimens from 80 NSCLC patients were collected from Affiliated Hospital of Chifeng University, which were frozen in liquid nitrogen immediately. The study was approved by the Ethics Committee Board of Affiliated Hospital of Chifeng University, and the written informed consent was obtained from each patient in accordance with institutional guidelines.

Cell transfection

The short hairpin RNA (shRNA) targeting FNDC1 (shFNDC1) or a negative control (shNC) was synthesized by Suzhou GenePharma Co., Ltd (Suzhou, China) and subcloned into lentivirus plasmids. For lentivirus production, the lentiviral vector, packaging plasmid (pAX2), and VSV-G envelope plasmid (pMD2.G) were co-transfected into HEK-293T cells by Lipofectamine 2000 (Thermo Fisher Scientific) according to the manufacturer's instructions. 48 h after the transfection, the supernatants of HEK-293T cells containing the lentiviral particle were collected and filtered through a 0.45 μm membrane. For NSCLC cell infection, 2×10^6 cells were seeded into a 6-well plate and grown to 60-70% confluency. Cells were infected with the corresponding recombinant lentivirus at a multiplicity of infection (MOI) =5 in the presence of 10 μg/mL polybrene. Infected cells were selected with 3 μg/mL puromycin (Sigma-Aldrich, St. Louis, MO, USA) for two weeks to eliminate the uninfected cells before further experiment. Western blotting and qRT-PCR were used to measure the knockdown efficiency.

Cell viability assay

NSCLC cells infected with lentivirus carrying shRNA targeting FNDC1 or control shRNA were seeded in to a 96 -well plate at a density of 1500 cell/well and cultured in a humidified cell culture incubator for 0, 24, 48, and 72 h, respectively. Subsequently, 10 μL CCK8 reaction solution (Solarbio Science & Technology Co., Ltd., Beijing, China) was added to the cell culture at indicated time point and the cells were further incubated for 3 h in a humidified cell culture incubator. The medium was then removed, and samples in each well were dissolved in 150 μL DMSO for 15 min at 37°C. The optical value of each sample at 450 nm was recorded with a multifunctional microplate reader (BioTek Instruments, Winooski, VT, USA).

Tube formation assay

An *in vitro* angiogenesis assay kit (ab204726; Abcam, Cambridge, UK) was employed for tube formation assay. In brief, 50 μL extracellular matrix (ECM) solution was added to a pre-chilled 96-well culture plate for 15-min coating at 37°C; 2.0×10^4 cells in DMEM with 10% (FBS) were seeded to each well for 18-h incubation. Cell morphology was then observed with a phase-contrast microscope (Leica, Wetzlar, Germany). The Image J Angiogenesis Analyzer (National Institutes of Health, Bethesda, MD, USA) was used for quantification of the network structure.

Migration and invasion assay

Transwell system (Corning, Inc., Corning, NY, USA) without matrigel pre-coating was applied for cell migration assay. Two (2) x 10^5 cells suspended in 350 μL serum-free medium were loaded into the upper chamber. Five hundred (500) μL complete medium

Non-commercial use only

was added into the bottom chamber. The cells were then cultured for 48 h, followed by the fixation with 4% paraformaldehyde at room temperature for 10 min and the staining with 0.5% crystal violet (Beyotime Institute of Biotechnology, Jiangsu, China) for 20 min. The migrating cells on the insert were photographed and counted from 5 randomly selected fields in each sample. For the cell invasion assay, transwell assay inserts (8 μm; Corning, Inc.) were coated with 1% matrigel. The upper insert was filled with serum-free medium containing 2×10^5 cells, while the bottom chamber was loaded with 500 μL complete medium. After 48 h, invading cells on the membrane were fixed in 4% paraformaldehyde and stained with 0.5% crystal violet (Beyotime) for 10 min. The invading cells were photographed and counted from 5 randomly selected fields in each sample.

EDU incorporation analysis

Cells were seeded into a 96-well plate at the density of 5000 cells/well. Click-iT™ EdU Cell Proliferation Kit for Imaging, Alexa Fluor™ 555 (Thermo Fisher Scientific) was used to detect cell proliferation. Prewarmed the 2x EdU solution was mixed (1:1 ratio) with the cell culture medium, and the cells were pulsed for 2 h. Cells were washed twice with PBS, followed by fixation with 100 μL of 3.7% formaldehyde 15 min at room temperature. After the removal of fixative solution, cells were washed twice with 100 μL of PBS with 3% BSA. Then 100 μL of 0.5% Triton® X-100 in PBS was added to each well for 20-min incubation. After the removal of Triton® X-100 solution, 1 x Click-iT® reaction cocktail was prepared based on the manufacturer's instruction and added to cells for 30-min incubation. The staining cocktail was removed and cells were counterstained by 500 nM DAPI for 10 min. After washing with PBS, and the images were captured under a fluorescence microscope (Leica).

Dual luciferase reporter assay

To demonstrate the functional interaction between miR-143-3p and FNDC1 mRNA, the wild type binding sequence or the mutated sequence was cloned into the PmirGLO vector expressing firefly luciferase (Promega, Madison, WI, USA). The reporter plasmid was co-transfected into 293T cells with either miRNA mimic or miR-NC in a 96-well plate (6000 cells/well) using lipofectamine 2000 reagent according to the manufacturer's instructions; 48 h post transfection, the relative luciferase activities were measured using dual-Luciferase reporter assay Kit (Promega) on a microplate reader (BioTek Instruments). The relative firefly luciferase activity in the reporter plasmid was normalized to that of Renilla luciferase (hRlucneo) control plasmid.

Western blot

Total protein was extracted from tissue and cell samples using RIPA lysis buffer containing protease inhibitor cocktail (Thermo Fisher Scientific). Cells suspended in RIPA buffer were lysed on ice for 10 min and lysed cells were centrifuged at 14,000 x g for 10 min. The concentration of obtained supernatant sample was measured using a Bradford assay kit (Beyotime Institute of Biotechnology). Fifteen (15) μg of total protein in each sample was denatured at 95°C for 10 min and loaded into a 10% or 12% SDS-PAGE gel. After separation, the protein bands were transferred onto a NC membrane (EMD Millipore), which was blocked with 5% milk at room temperature for 1 h. The membrane was probed with primary antibodies at 4°C for 18 h: FNDC1 (PA5-56603, 1:1000 dilution); GAPDH (#5174, 1:2000 dilution; Cell Signaling Technology Inc., Danvers, MA, USA), vimentin (ab92547, 1:1000 dilution; Abcam), N-cadherin (ab76011, 1:1000 dilution; Abcam), E-cadherin (ab40772, 1:1000 dilution; Abcam), VEGFA (ab52917, 1:1000 dilution; Abcam). The membrane was washed with TBST buffer (Beyotime Institute of Biotechnology) and then incubated with HRP-conjugated secondary antibodies (Cell Signaling Technology Inc.; anti-mouse secondary antibody, # 7076; and anti-rabbit secondary antibody; #7074, both at 1:2500 dilution) at room temperature for 1 h. Signal development was conducted using an ECL Prime Western blotting kit (Bio-Rad Lab., Hercules, CA, USA). The protein bands were photographed on a gel imager system (Bio-Rad), and the densitometry analysis of band intensity was performed with Image J software (NIH).

Xenograft mouse model

All animal procedures were approved by the Animal Care and Use Ethical Committee of Affiliated Hospital of Chifeng University. Twelve male nude mice weighing 30-40 g were housed in specific pathogen-free conditions on a 12-h light/dark cycle. The mice were randomly assigned into two groups (6 mice in each group): sh-NC group (injected with H1299 cells infected with lentivirus carrying sh-NC), (2) sh-FNDC1 (injected with H1299 cells infected with lentivirus carrying sh-FNDC1); 0.2 mL of cell suspension containing 2×10^6 cells were injected into the right flank of each mice. Tumor volumes were monitored 7, 14, 21, and 28 days post-injection respectively, using a caliper and the following formula: tumor volume = 0.5 × length × width^2. On day 28, the mice were euthanized by CO_2 asphyxiation and subsequent cervical dislocation. The tumors of terminally dead mice were resected for weight measurement and further analysis. The lung tissue was also collected for metastasis analysis.

Hematoxylin and Eosin (H&E) staining

H&E staining was performed using H&E Stain Kit (ab245880, Abcam). The tissues were fixed with paraformaldehyde and then embedded in paraffin. The tissue blocks were cut into 5 μm sections using a microtome. For deparaffinization and re-hydration, the sections were subjected to three washes of xylene for 5 min each, two washes of 100% ethanol for 10 min each, two washes of 95% ethanol for 10 min each, and two washes in distilled water for 5 min each. Deparaffinized/hydrated section of the lung tissues was incubated in adequate Mayer's hematoxylin solution to completely cover tissue section for 5 min. The section was rinsed twice with distilled water to remove excess stain. Then adequate Bluing reagent was applied to cover tissue section for 30 sec. After washing with distilled water, the section was dehydrated in absolute alcohol, followed by staining with Eosin Y solution for 2 min. The section was rinsed using absolute ethanol for three times and then mounted to a slide. The images were collected under an inverse microscope (Leica).

Immunohistochemistry

The tumor tissues sections were prepared as described in the H&E section. After deparaffinization and rehydration, the sections were subjected to antigen retrieval by heating the section in a microwave submersed in 1x citrate unmasking solution (SignalStain® Citrate Unmasking Solution, 10x, #14746; Cell Signaling Technologies, Inc.). The heating was performed at a sub-boiling temperature (95-98°C) for 10 min. Sections were cooled on bench top for 30 min, and then incubated in 3% hydrogen peroxide for 10 min at 25°C. After three times washes in TBST buffer for 5 min, the sections were blocked with 5% normal goat serum (Sigma-Aldrich) for 1 h and then incubated with primary antibody (anti-Ki67, ab15580, 1:300 dilution; Abcam); anti-FNDC1, PAB22769, 1:300 dilution; Amyjet Scientific, Wuhan, China) overnight at 4°C. The rabbit IgG isotype (ab270144, 1:300 dilution, Abcam) was used as the staining control for the background signal. The sections were washed three times using TBST buffer for 5 min each, and then incubated with 300 μL SignalStain® Boost Detection Reagent (HRP, rabbit #8114; Cell Signaling Technologies, Inc.) for 30 min at room temperature.

Non-commercial use only

OPEN ACCESS

Signal development was performed using 400 µL SignalStain® substrate (#8059; Cell Signaling Technologies, Inc.) and the nuclei were counter-stained with hematoxylin before imaging. The positive staining signaling was assessed using the IgG isotype negative controls as the background reference. There were 6 tumor samples (n=6 mice) processed in each group, at least 5 sections were analyzed for each tumor samples.

Data analyses using online tools

Starbase (https://www.hsls.pitt.edu/obrc/index.php?page= URL 20110217163843), Targetscan (https://www.targetscan.org/vert_72/), miRDB (http://mirdb.org/) as well as miRWalk (http://mirwalk.umm.uni-heidelberg.de/) were used in our study for predicting the miRNA regulators of FNDC1. The associations of overall survival in patients with different FNDC1 expression level

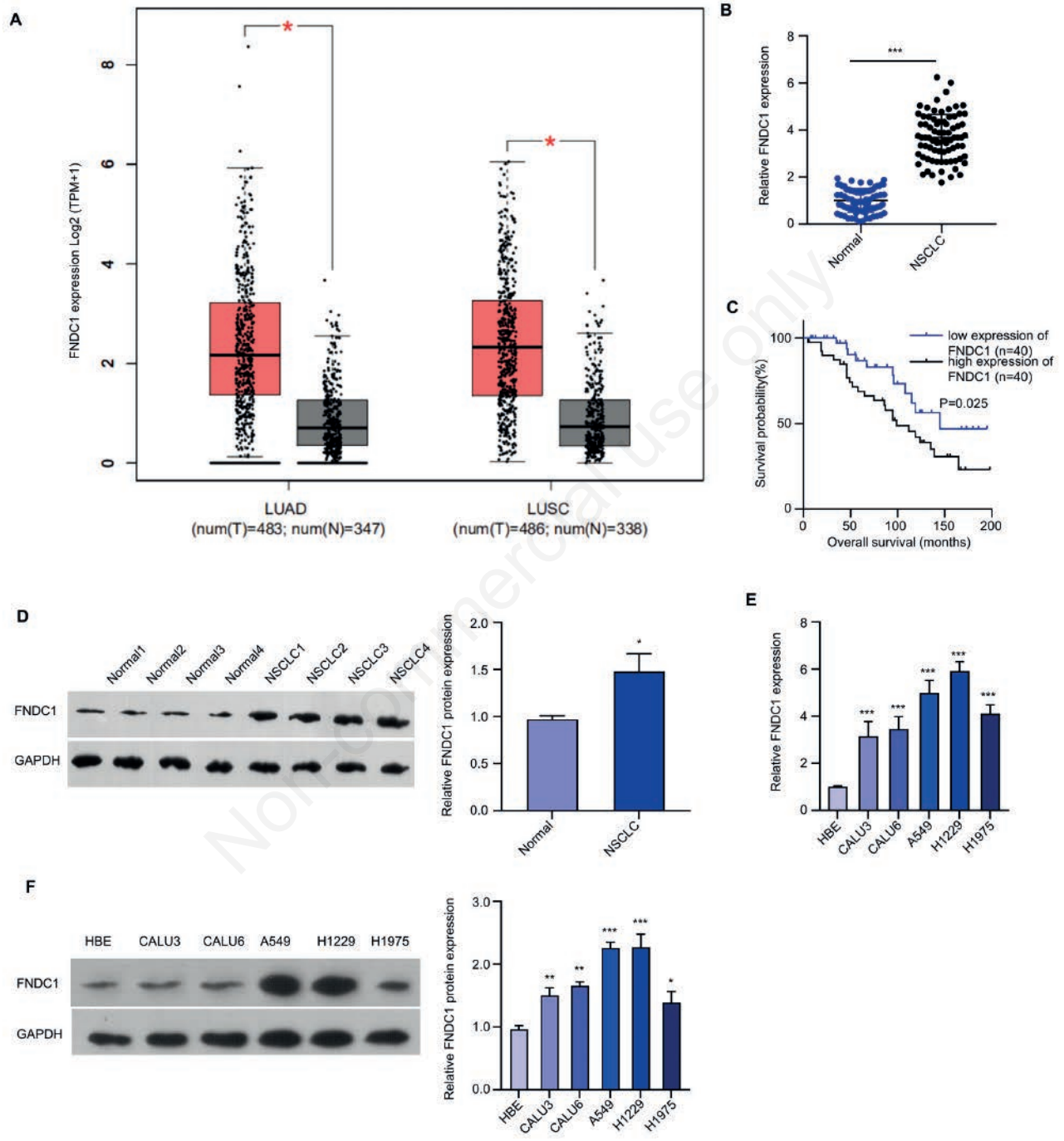

Figure 1. The upregulation of FNDC1 in NSCLC tumor tissues and cell lines. A) FNDC1 expression in Lung squamous cell carcinoma (LUSC), lung adenocarcinoma (LUAD) and the adjacent normal tissues from TCGA database. B) The mRNA level of FNDC1 was determined by qRT-PCR in NSCLC tumor and adjacent normal tissues of NSCLC patients (n=80, p<0.001). C) The overall survival rate of NSCLC patients in FNDC1-high and low-expression groups by Kaplan Meier analysis. D) The protein level of FNDC1 in 4 cases of NSCLC tumor and adjacent tissues was examined by Western blot. E) The mRNA levels of FNDC1 in NSCLC cell lines (h1229, calu3, h1975, calu6, A549) and human bronchial epithelial cells (HBE) were examined by qRT-PCR. F) The protein levels of FNDC1 in NSCLC cell lines and HBE cells were detected by Western blot.

Non-commercial use only

was analyzed *via* K-M plotter (https://kmplot.com/analysis/), with the median FNDC1 expression level as the cut-off for high- and low-expression groups. For all the online tools, we used the default setting for our data mining.

RNA extraction and qRT-PCR

Total RNA samples from NSCLC tissues and cells were extracted using Trizol reagent (Thermo Fisher Scientific) based on the supplier's instructions; 5 μg of total RNA was used for reverse-transcription into cDNA using RevertAid First Strand cDNA Synthesis Kit (Thermo Fisher Scientific). The cDNA was quantified by qPCR using BlazeTaq™ SYBR Green qRT-PCR Mix (Takara) on the CFX96 Touch qPCR system (Bio-Rad). The following cycling condition was used: 95°C 2 min, 40 cycles of 95°C 30 s,

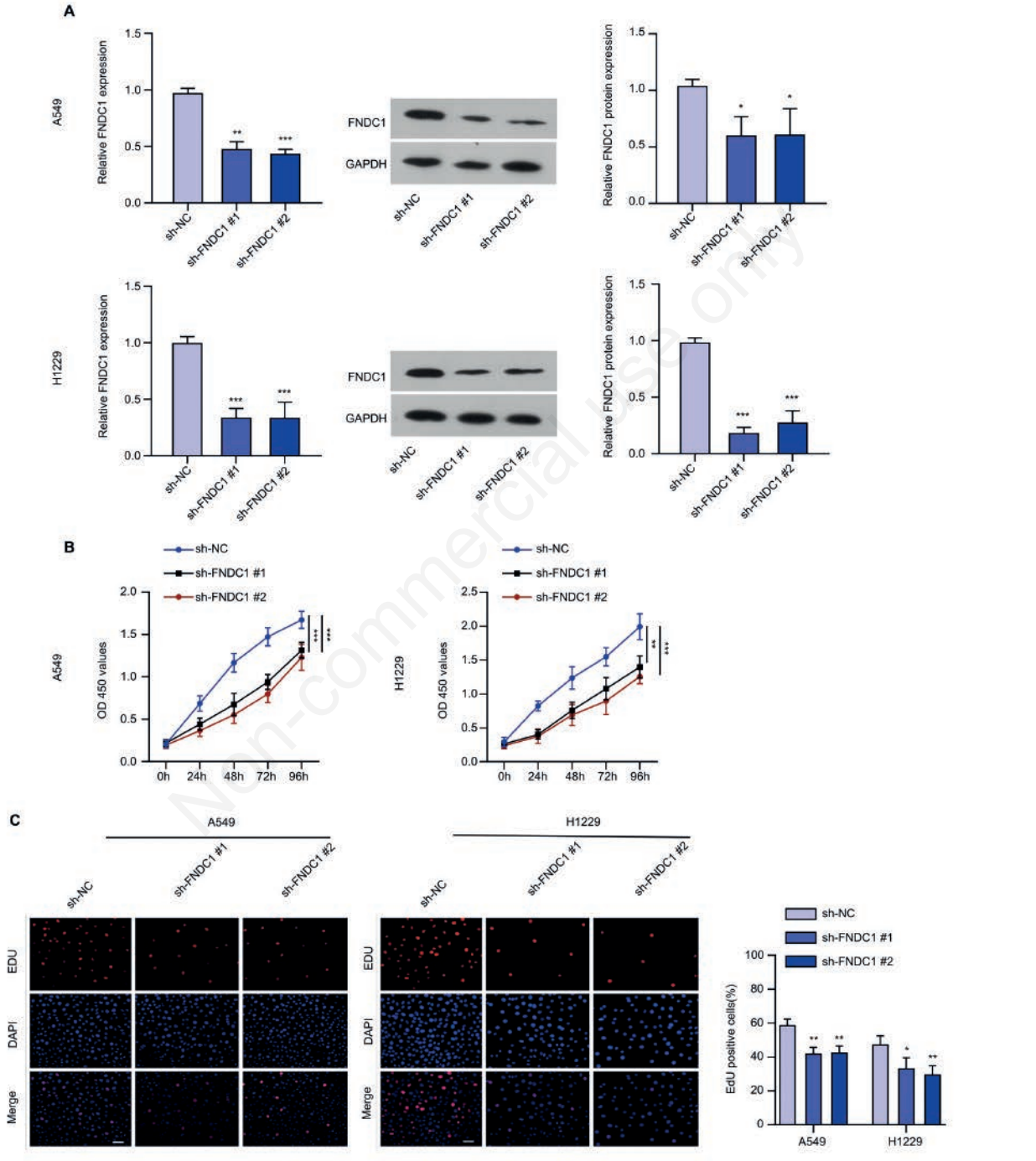

Figure 2. Downregulation of FNDC1 inhibited the proliferation of NSCLC cells. A) FNDC1 knockdown in A549 and h1229 cells by two shRNAs (sh-FNDC1 #1, #2) and the knockdown efficiency was detected by Western blot and qRT-PCR. B) CCK-8 proliferation assay in A549 and h1229 cells stably expressing sh-NC, sh-FNDC1 #1, and #2. C) EDU incorporation staining of proliferating cells in A549 and h1229 cell line stably expressing sh-NC, sh-FNDC1 #1, and #2. Scale bar: 50 μm.

Non-commercial use only

60°C 30 s and 70°C 60 s. Standard method ($2^{-\Delta\Delta CT}$) was employed to analyze the relative expression of each target. Primer sequences used in this study: hsa-miR-143-3p (forward: TGAGATGAAGCAC TGTAGCTC, reverse: GAGCTACAGTGCTTCATCTCA), U6 (forward: CTCGCTTCGGCAGCACA, reverse: AACGCTTCA CGAATTTGCGT), GAPDH (forward: CCTGCACCACCAAC TGCTTA, reverse: GGCCATCCACAGTCTTCTGAG), FNDC1 (forward: CAACATTGCCTATGGGAAGTCA, reverse: CTCGA TCCATTCACCTCCAG).

Statistical analysis

Statistical analyses in this study were performed with GraphPad Prism version 8.0 (GraphPad software). The data were expressed as the mean ± standard deviation. Unpaired Student's *t*-test was used for two-group comparisons and one-way ANOVA with Tukey's *post-hoc* test was employed for multiple comparisons. The association between FNDC1 expression level and clinicopathological data of NSCLC patients was investigated by Chi-square test.

Results

FNDC1 was upregulated in NSCLC tissues and cell lines

To explore the potential role of FNDC1 in NSCLC, we searched TCGA database for the lung cancer patients of containing lung squamous cell carcinoma (LUSC), lung adenocarcinoma (LUAD) and the adjacent normal tissues, and compared the expression levels of FNDC1 in the tumor and normal tissues. It was found that FNDC1 was significantly upregulated lung tumor tissues of both LUSC and LUAD, compared to normal tissues (Figure 1A). We also collected tumor tissues and normal tissues from 80 NSCLC patients and analyzed FNDC1 expression pattern, which validated the overexpression of FNDC1 in NSCLC (Figure 1B). The 80 NSCLC patients were divided into FNDC1 low-expression (n=40) and high-expression group (n=40) based on the median expression value of FNDC1. The overall survival analysis of the two groups by Kaplan Meier curve demonstrated a poorer prognosis in FNDC1 high-expression group (Figure 1C). Western blot analysis confirmed the elevated protein level of FNDC1 in NSCLC tumor samples compared to the adjacent ones (Figure 1D). Further, the increase of FNDC1 expression at mRNA and protein level was also found in NSCLC cell lines (calu6, A549, calu3, h1229, h1975) when compared to human bronchial epithelial cells (HBE) (Figure 1 E,F). We also analyzed the association between

FNDC1 level and clinicopathological data of NSCLC patients by Chi-square test (Table 1). High FNDC1 level was associated with advanced TNM stage and distal node metastasis in NSCLC patients. Together, these findings unveil the significance of FNDC1 overexpression in NSCLC, suggesting FNDC1 as a potential oncogenic factor in NSCLC.

Knockdown of FNDC1 inhibited the proliferation of NSCLC cells

To investigate the functional roles of FNDC1 in NSCLC cells, we used two shRNAs (stable strains were constructed by lentivirus) to silence FNDC1 expression. Compared with control cells (sh-NC), sh-FNDC1 #1 and #2 could effectively reduce FNDC1 level in A549 and h1229 lines (Figure 2A). As revealed by CCk-8 proliferation assay, silencing FNDC1 could impair the proliferation of NSCLC cells (Figure 2B). Consistently, knockdown of FNDC1 suppressed the DNA synthesis rate of NSCLC cells, as shown by the reduced number of EDU incorporating cells (Figure 2C). These data indicated that FNDC1 is required for sustaining the proliferation in NSCLC cells.

Non-commercial use only

Table 1. Correlation between FNDC1 expression and clinicopathological characteristics of non-small cell lung cancer patients.

Clinicopathological characteristics	Total	FNDC1 expression		p
		High	Low	
Gender				
Male	36	19	17	0.653
Female	44	21	23	
Age (years)				
≤60	45	21	24	0.499
>60	35	19	16	
Tumor size				
T1	22	10	12	0.922
T2	19	9	10	
T3	19	10	9	
T4	20	11	9	
Distant metastasis				
Positive	44	31	13	0.001***
Negative	36	9	27	
Differentiation				
High	30	14	16	0.875
Moderate	20	10	10	
Poor	30	16	14	
TNM stages				
I	19	14	5	0.002**
II	16	7	9	
III	14	6	8	
IV	21	3	18	

TNM, overall stage to describe the tumor (T), node (N), and metastasis (M) categories; **p<0.01, ***p<0.001.

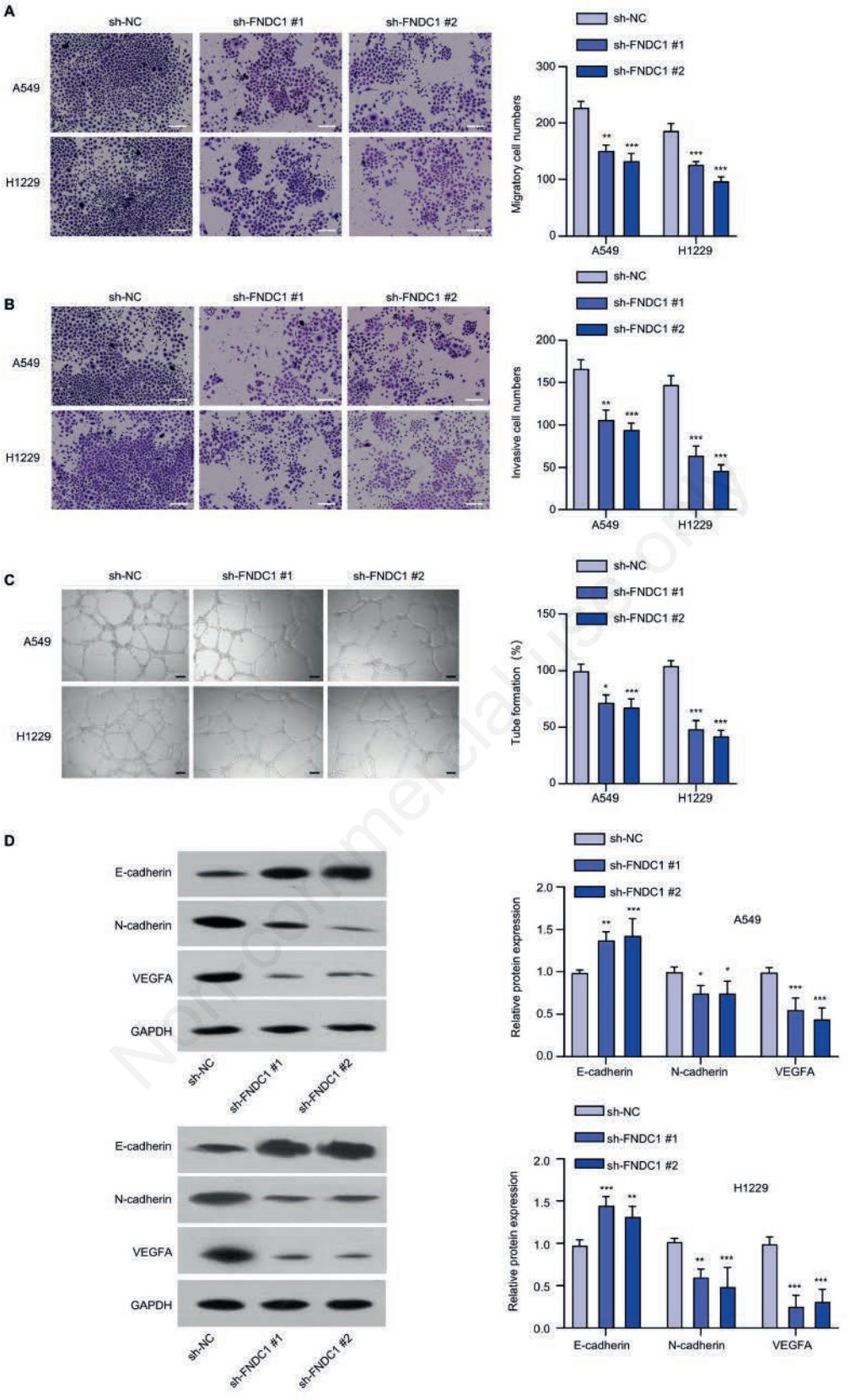

Figure 3. **Silencing FNDC1 suppressed the migration, invasion, EMT and angiogenic potential of NSCLC cells. A) Transwell migration assay in A549 and h1229 cell line stably expressing sh-NC, sh-FNDC1 #1, and #2; scale bar: 250 μm. B) Transwell invasion assay in A549 and h1229 cell line stably expressing sh-NC, sh-FNDC1 #1, and #2; scale bar: 250 μm. C) *In vitro* tube formation assay in A549 and h1229 cell line stably expressing sh-NC, sh-FNDC1 #1, and #2; scale bar: 50 μm. D) The protein levels of E-cadherin, N-cadherin and VEGFA in A549 and h1229 cell line stably expressing sh-NC, sh-FNDC1 #1, and #2.**

Non-commercial use only

OPEN ACCESS

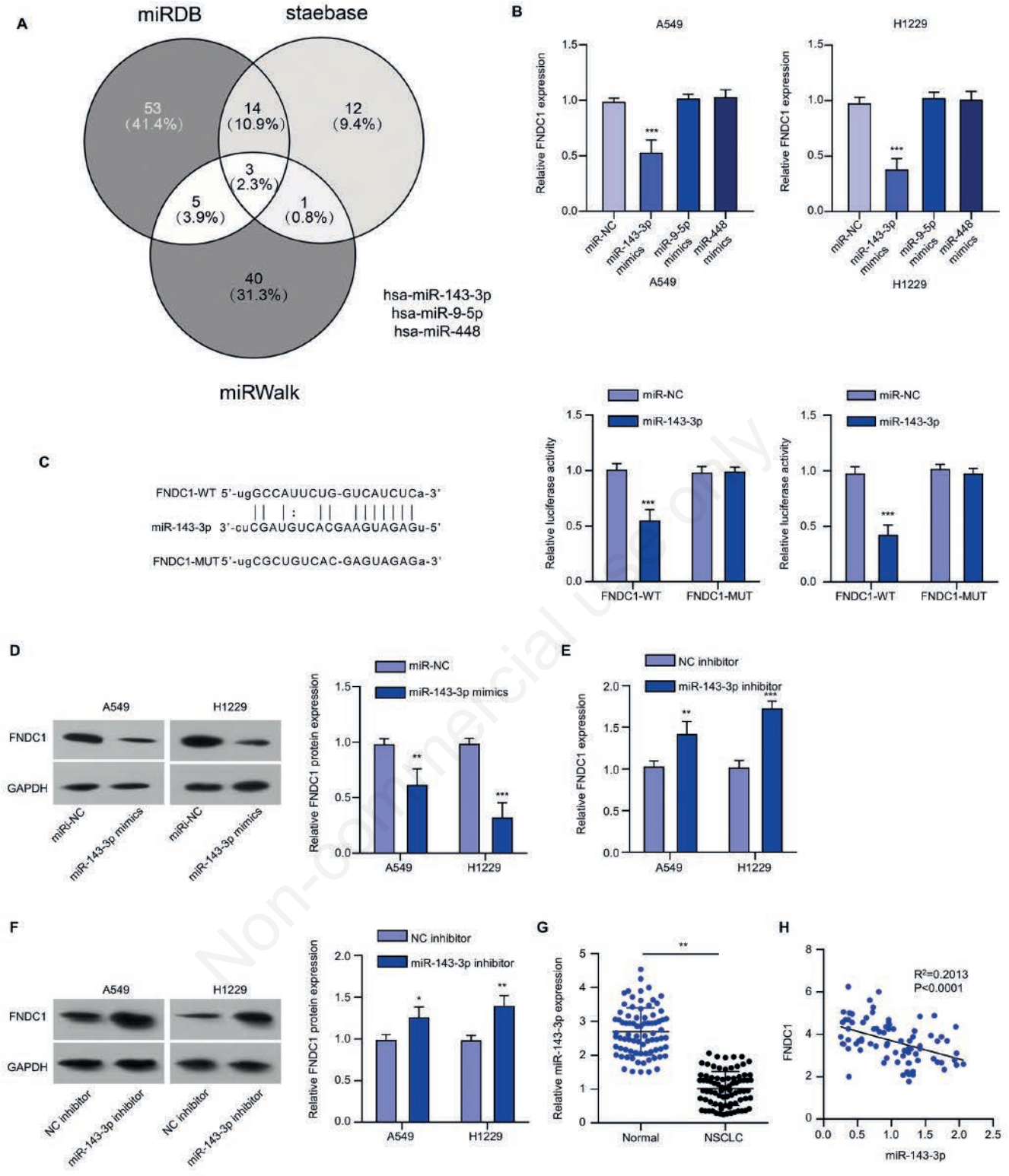

Figure 4. miR-143-3p negatively targets FNDC1. A) "Starbase", "miRDB" and "miRWalk" miRNA database was utilized to predict the predicted the candidate miRNAs of FNDC1; three common candidates were identified: hsa-miR-143-3p; hsa-miR-9-5p; hsa-miR-448. B) Cells were transfected with miR-NC, miR-143-3p mimic, miR-9-5p mimic, or miR-448 mimic, respectively; FDNC1 expression was detected by qRT-PCR 48 h after transfection. C) Dual luciferase reporter assay using FDNC1-WT or MUT reporter in the presence of miR-143-3p mimic or miR-NC. D) The protein level of FNDC1 was analyzed by Western blot after the transfection of miR-NC or miR-143-3p mimic. E) The RNA level of miR-143-3p after the transfection of NC inhibitor or miR-143-3p inhibitor. F) The protein level of FNDC1 after the transfection of NC inhibitor or miR-143-3p inhibitor. G) The expression level of miR-143-3p in tumors tissues and adjacent normal tissues of NSCLC patients (n=80, p<0.001). H) The correlation of FNDC1 and miR-143-3p expression in NSCLC tumor samples (n=80, p<0.001).

Non-commercial use only

Knockdown of FNDC1 repressed the migration, invasion, epithelial-mesenchymal transition and *in vitro* angiogenesis of NSCLC cells

To further study the impact of FNDC1 silencing on the malignancy of NSCLC cells, we performed cell migration and invasion upon FNDC1 knockdown. As shown in Figure 3 A,B, the knockdown of FNDC1 inhibited the migratory and invasive capacity of NSCLC cells. In the tube formation, silencing FNDC1 also suppressed the angiogenic potential of NSCLC cells (Figure 3C). As cell migration and invasion is related to the epithelial-

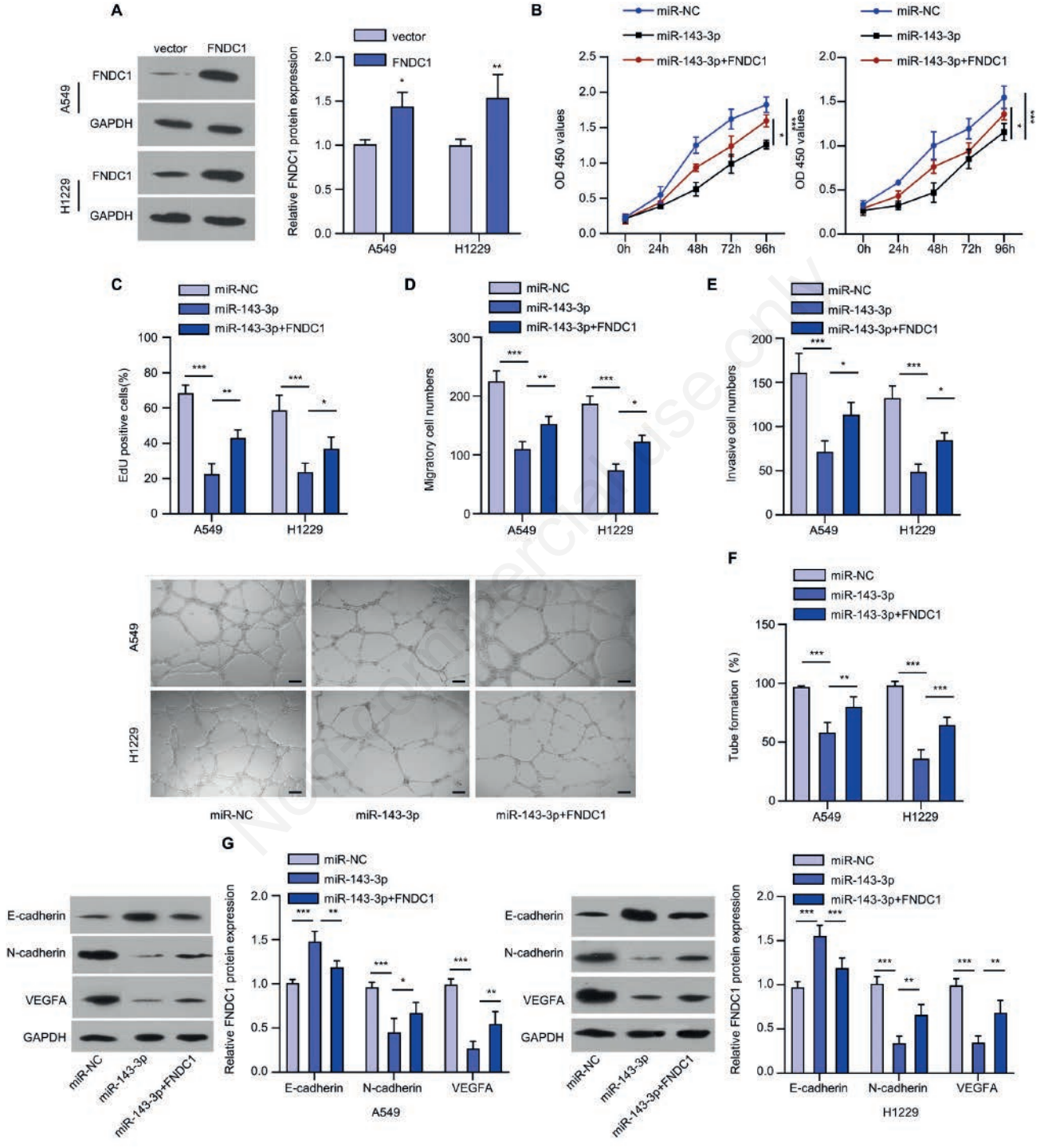

Figure 5. FNDC1 overexpression partially reversed the effect of miR-143-3p mimic on the malignancy of NSCLC cells. A) The protein level of FNDC1 in A549 and H1229 cells transfected with empty vector or FNDC1 expression vector. B) CCK-8 assay in cells transfected with miR-NC, miR-143-3p mimic or miR-143-3p mimic plus NDC1 expression vector. C) EDU staining in above experimental conditions. D,E) Transwell migration and invasion assay in above experimental conditions. F) *In vitro* tube formation in above experimental conditions; scale bar: 50 μm. G) E-cadherin, N-cadherin and VEGFA protein levels in above experimental conditions.

mesenchymal transition (EMT), we next measured EMT markers by Western blot. As shown in Figure 3D, knockdown of FNDC1 increased the protein expression of E-cadherin (epithelial marker), while the protein levels of N-cadherin (mesenchymal marker) and VEGF-A (angiogenic factor) were reduced. Taken together, these results suggest FNDC1 promotes the migration, invasion, EMT and angiogenic potential of NSCLC cells.

MiR-143-3p could negatively regulate FNDC1 expression

Generally, miRNAs are important regulator of protein level in the progression of cancers. We next sought to seek for the miRNA regulator of FNDC1. With the prediction of three public databases (Starbase, miRDB and miRWalk), we found three common candidate miRNAs which could potentially regulate FNDC1: hsa-miR-143-3p; hsa-miR-9-5p; hsa-miR-448 (Figure 4A). Among them, we focused on the analysis of miR-143-3p, since only miR-143-3p mimic could significantly repress FNEC1 expression (Figure 4B). Dual luciferase reporter assay revealed that, compared with miR-NC, the transfection of miR-143-3p mimic was able to repress the luciferase activity in the WT reporter of FNDC1, while this inhibition was abolished in the MUT reporter of FNDC1, indicating that the two molecules interact with each other *via* wild type binding sites (Figure 4C). The transfection of miR-143-3p mimic also reduced FNDC1 expression at protein level (Figure 4D). We also used miR-143-3p inhibitor to downregulate miR-143-3p in A549 and h1229 cells (Figure 4E). In contrast to miR-143-3p mimic, FNDC1 protein level was increased upon the transfection of miR-143-3p inhibitor (Figure 4F). To investigate miR-143-3p expression pattern in NSCLC samples, the RNA level of miR-143-3p in 80 cases of NSCLC tumor and adjacent normal tissues was measured by qRT-PCR, which revealed the significant downregulation of miR-143-3p in NSCLC tumors (Figure 4G). There was also a significant negative association between the expression of FNDC1 and miR-143-3p (Figure 4H). Overall, our data suggest that miR-143-3p interact with FNDC1 mRNA to negatively regulate its expression.

Overexpression of FNDC1 partially rescued the effect of miR-143-3p mimic in NSCLC cells

In order to prove the regulator miR-143-3p/FNDC1 axis in NSCLC cells, we applied FNDC1 overexpression plasmid to increase FNDC1 in A549 and H1229 cells (Figure 5A). Then the cells were transfected with miR-NC, miR-143-3p mimic or miR-143-3p mimic plus FNDC1 expression vector. CCK8 assay showed that miR-143-3p mimic could suppressed cell proliferation, and the co-transfection of FNDC1 plasmid partially restored cell proliferation (Figure 5B). Similarly, miR-143-3p mimic reduced the EDU-positive cells, and FNDC1 overexpression increased EDU-positive cells (Figure 5C). Migration and invasion ability of NSCLC cells in different groups were determined by transwell assays with or without the Matrigel coating. miR-143-3p mimic inhibited the migratory and invasive abilities of NSCLC cells, and FNDC1 overexpression partially enhanced cell migration and invasion in the presence of miR-143-3p mimic (Figure 5 D,E). Similar rescue effect was observed for the angiogenic potential in the tube formation assay (Figure 5F). Lastly, we examined EMT marker by Western blot in different experimental groups. The transfection of miR-143-3p mimic dramatically decreased the expression of N-cadherin and VEGFA, while the expression level of E-cadherin was increased. However, the co-transfection of FNDC1 plasmid partially reversed the effects of miR-143-3p mimic on N-cadherin, E-cadherin and VEGFA levels (Figure 5G). Taken together, these results indicate that miR-143-3p/FNDC1 axis regulates the malignant phenotype in NSCLC cells.

Knockdown of FNDC1 suppressed tumor formation and metastasis of NSCLC cells *in vivo*

To investigate the *in vivo* role of FNDC1 in NSCLC, xenograft mouse model was established using H1299 cells stably expressing sh-NC or sh-FNDC1. The tumor growth measurement showed the tumor-suppressive effect of FNDC1 silencing *in vivo* (Figure 6 A,B). Compared with sh-NC group, the knockdown of FNDC1 significantly reduced tumor volume and tumor weight. Ki-67 is a proliferative marker.[16] The immunohistochemical staining of Ki-67 and FNDC1 showed that, in the sh-FNDC1 groups with the downregulation of FNDC1, the expression level of Ki-67 was also significantly repressed (Figure 6C), indicating the proliferation-suppressive effect of FNDC1 knockdown *in vivo*. In addition, FNDC1 silencing also suppressed the EMT by downregulating N-cadherin and VEGFA and upregulating E-cadherin (Figure 6D). Consistent with this, H&E staining in the lung tissues revealed reduced lung metastatic nodules in the mice injected with FNDC1 silencing cells (Figure 6 E,F).

Discussion

The functions of extracellular matrix related proteins in the progression of cancer have attracted increasing research attention.[6] For instance, fibronectin dysregulation was implicated in the progression of gastric cancer.[17] Structural domain of FNDC1 was reported to be a pathogenic factor leading to acute otitis.[12] Additionally, FNDC1 is involved in the regulation of cardiomyocyte apoptosis under hypoxia.[17,18] Similarly, FNDC1 also contributes to hypermethylation-induced apoptosis in human salivary gland adenoid cystic carcinoma.[19] Our study reported the overexpression of FNDC1 in NSCLC tumor samples and cancer cell lines. Its knockdown not only undermines the malignant phenotype of NSCLC cells, but also impairs tumor growth and metastasis in the animal model. Thus, our data provide solid evidence supporting the oncogenic role of FNDC1 in NSCLC.

Previous studies suggest that FNDC1 level could be modulated by miRNAs in cancers. For example, miR-1207-3p/FNDC1 axis is implicated in prostate cancer. The increased expression of miR-1207-3p shows inhibitory effects on the migration and proliferation of prostate cancer cells by targeting FNDC1.[14] However, the specific mechanism of FNDC1 overexpression in NSCLC remains to be elucidated. Lung cancer is a heterogeneous disease and their multiple factors implicated in its malignant progression. Understanding the molecular mechanisms responsible for the malignancy of NSCLC is essential for the development of effective therapies. Challenges in Lung cancer or NSCLC management also include the lack of reliable diagnostic and prognostic biomarkers. In present study, reported that the heightened FNDC1 level was correlated with the dismal prognosis in NSCLC patients, indicating its potential as a prognostic marker. Importantly, we also identified miR-143-3p as a negative regulator of FNDC1. miR-143-3p was downregulated in NSCLC tumor and cell lines, and its overexpression attenuate the malignant phenotype of NSCLC cells. These data suggest that miR-143-3p serves as a tumor-suppressor in NSCLC cells, although its tumor-suppressive effect needs to be further validated in animal model.

miRNAs plays important roles in post-transcriptional regulation of protein expression. Different miRNAs may serve as either oncogenic factors or tumor suppressors across cancer types.[20] miRNAs could repress target gene expression through binding to the 3′UTR (untranslated region) of mRNA. In this study, we confirmed the interaction of miR-143-3p with FNDC1 mRNA 3'UTR in NSCLC cells. Moreover, miR-143-3p was downregulated

Non-commercial use only

in NSCLC tissues and its expression level was conversely correlated with FNDC1 expression. A previous study has reported that miR-143-3p was downregulated in bladder cancer, and its reduced level was associated with the poor prognosis of bladder cancer patients.[21] In addition, the downregulation of miR-143 was also found in cervical cancer, and its overexpression inhibited tumor cell growth through targeting Bcl-2.[22] Furthermore, miR-143-5p could downregulate COX-2 in gastric cancer to induces apoptosis and undermine cell survival.[23] We showed that miR-143-3p overexpression not only suppressed cell growth, but also impaired the migration and invasion of NSCLC cells by attenuating EMT. Thus, our data and previous evidence altogether support the tumor-suppressive function of miR-143-3p in different cancer. Nevertheless, the mechanisms underlying miR-143-3p downregulation in NSCLC tumors need to be investigated in future studies. We surmise that other non-coding RNAs such as lncRNAs or circRNAs may function as upstream regulators governing the expression of miR-143-3p.

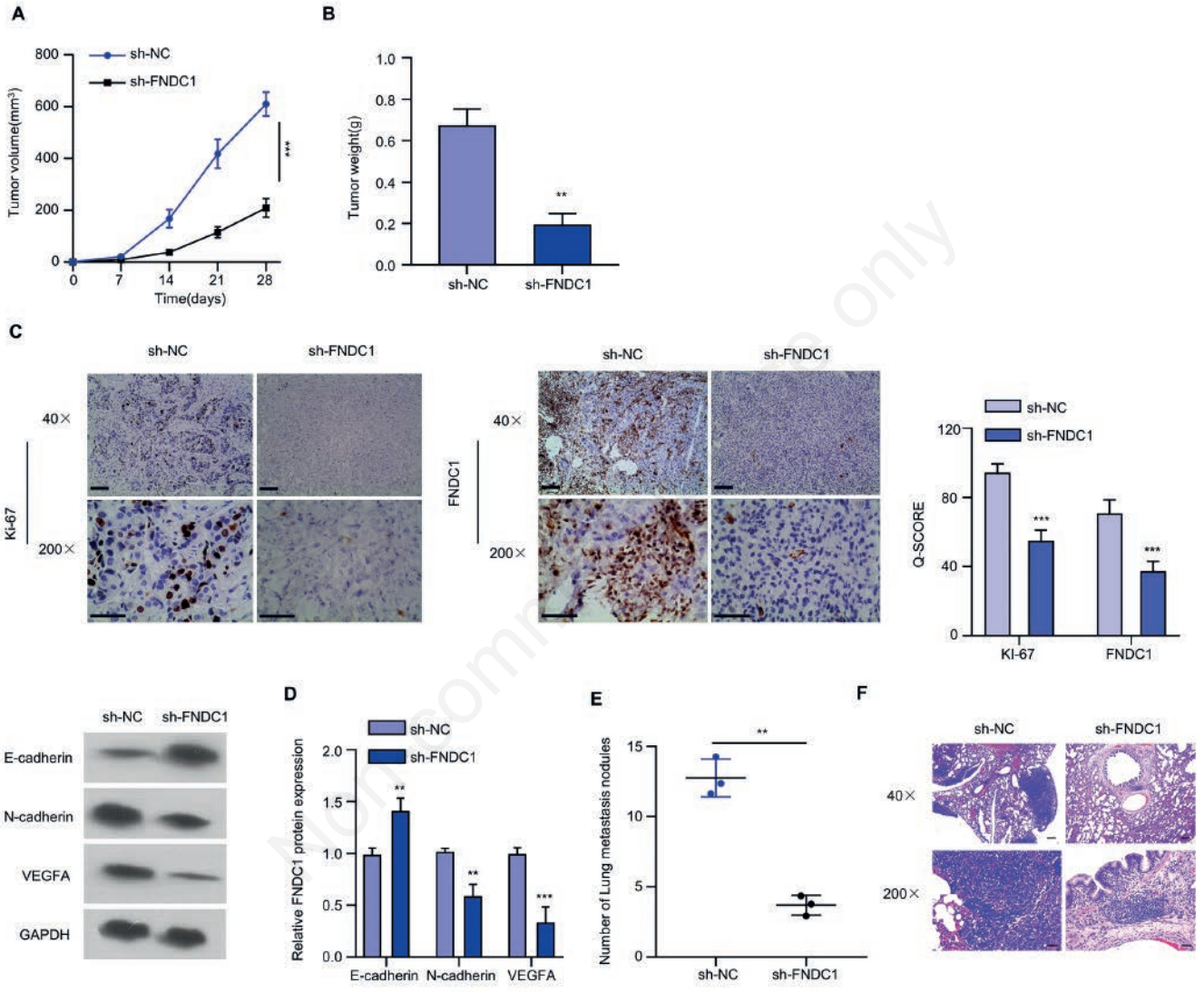

Figure 6. Knockdown of FNDC1 suppresses cell proliferation and metastasis of NSCLC cells *in vivo*. A) H1299 cells stably expressing sh-NC or sh-FNDC1 were inoculated into nude mice, and the tumor volume was measured every 7 days (n=6 in each group). B) The subcutaneous tumor mass was measured on day 28. C) immunohistochemical staining of Ki-67 and FNDC1 was performed in the tumor sections of sh-NC and sh-FNDC1 groups; scale bar: 200 μm (40x) and 100 μm (200x). D) The protein levels of E-cadherin, N-cadherin and VEGFA in the tumor tissues of sh-NC and sh-FNDC1 groups were measured by Western blot. E) The number of lung nodules in the lung tissue of sh-NC and sh-FNDC1 groups (n=6 in each group). F) H&E staining of the lung tissues of sh-NC and sh-FNDC1 groups. Representative images under 40x (scale bar: 180 μm) and 200x (scale bar: 40 μm) magnification.

Non-commercial use only

References

1. Bray F, Ferlay J, Soerjomataram I, Siegel RL, Torre LA, Jemal A. Global cancer statistics 2018: GLOBOCAN estimates of incidence and mortality worldwide for 36 cancers in 185 countries. CA Cancer J Clin 2018;68:394-424.
2. Zappa C, Mousa SA. Non-small cell lung cancer: Current treatment and future advances. Transl Lung Cancer Res 2016;5:288-300.
3. Dias M, Linhas R, Campainha S, Conde S, Barroso A. Lung cancer in never-smokers–what are the differences? Acta Oncologica 2017;56:931-5.
4. Sun S, Schiller JH, Gazdar AF. Lung cancer in never smokers - A different disease. Nat Rev Cancer 2007;7:778-90.
5. Lemjabbar-Alaoui H, Hassan OUI, Yang YW, Buchanan P. Lung cancer: biology and treatment options. Biochim Biophys Acta Rev Cancer 2015;1856:189-210.
6. Schabath MB, Cote ML. Cancer progress and priorities: lung cancer. Cancer Epidemiol Biomarkers Prev 2019;28:1563-79.
7. Raso MG, Behrens C, Herynk MH, Liu S, Prudkin L, Ozburn NC, et al. Immunohistochemical expression of estrogen and progesterone receptors identifies a subset of NSCLCs and correlates with EGFR mutation. Clin Cancer Res 2009;15:5359-68.
8. Wang DC, Wang W, Zhu B, Wang X. Lung cancer heterogeneity and new strategies for drug therapy. Annu Rev Pharmacol Toxicol 2018;58:531-46.
9. Lin TC, Yang CH, Cheng LH, Chang WT, Lin YR, Cheng HC. Fibronectin in cancer: friend or foe. Cells 2020;9:27.
10. Pankov R, Yamada KM. Fibronectin at a glance. J Cell Sci 2002;115:3861-3.
11. Albrecht M, Renneberg H, Möschler O, Janssen M, Aumüller G, Konrad L, et al. Fibronectin in human prostatic cells in vivo and in vitro: expression, distribution, and pathological significance. Histochem Cell Biol 1999;112:51-61.
12. Fernandez-Garcia B, Eiró N, Marín L, González-Reyes S, González LO, Lamelas ML, et al. Expression and prognostic significance of fibronectin and matrix metalloproteases in breast cancer metastasis. Histopathology 2014;64:512-22.
13. Anderegg U, Breitschwerdt K, Köhler MJ, Sticherling M, Haustein UF, Simon JC, et al. MEL4B3, a novel mRNA is induced in skin tumors and regulated by TGF-β and pro-inflammatory cytokines. Exp Dermatol 2005;14:709-18.
14. Das DK, Naidoo M, Ilboudo A, Park JY, Ali T, Krampis K, et al. miR-1207-3p regulates the androgen receptor in prostate cancer via FNDC1/fibronectin. Exp Cell Res 2016;348:190-200.
15. Jiang T, Gao W, Lin S, Chen H, Du B, Liu Q, et al. FNDC1 Promotes the invasiveness of gastric cancer via Wnt/β-catenin signaling pathway and correlates with peritoneal metastasis and prognosis. Front Oncol 2020;10:590492.
16. Menon SS, Guruvayoorappan C, Sakthivel KM, Rasmi RR. Ki-67 protein as a tumour proliferation marker. Clin Chim Acta 2019;491:39-45.
17. Liu YP, Chen WD, Li WN, Zhang M. Overexpression of FNDC1 relates to poor prognosis and its knockdown impairs cell invasion and migration in gastric cancer. Technol Cancer Res Treat 2019;18:153303381986992.
18. Taniguchi K, Sugito N, Kumazaki M, Shinohara H, Yamada N, Nakagawa Y, et al. MicroRNA-124 inhibits cancer cell growth through PTB1/PKM1/PKM2 feedback cascade in colorectal cancer. Cancer Letters 2015;363:17-27.
19. Bell A, Bell D, Weber RS, El-Naggar AK. CpG island methylation profiling in human salivary gland adenoid cystic carcinoma. Cancer 2011;117:2898-909.
20. Di Leva G, Garofalo M, Croce CM. MicroRNAs in cancer. Annu Rev Pathol 2014;9:287-314.
21. Lin T, Dong W, Huang J, Pan Q, Fan X, Zhang C, et al. MicroRNA-143 as a tumor suppressor for bladder cancer. J Urol 2009;181:1372-80.
22. Liu L, Yu X, Guo X, Tian Z, Su M, Long Y, et al. MiR-143 is downregulated in cervical cancer and promotes apoptosis and inhibits tumor formation by targeting Bcl-2. Mol Med Rep 2012;5:753-60.
23. Wu XL, Cheng B, Li PY, Huang HJ, Zhao Q, Dan ZL, et al. MicroRNA-143 suppresses gastric cancer cell growth and induces apoptosis by targeting COX-2. World J Gastroenterol 2013;19:7758-65.

Non-commercial use only

Received for publication: 12 October 2022. Accepted for publication: 22 March 2023.
This work is licensed under a Creative Commons Attribution-NonCommercial 4.0 International License (CC BY-NC 4.0).
©Copyright: the Author(s), 2023
Licensee PAGEPress, Italy
European Journal of Histochemistry 2023; 67:3577
doi:10.4081/ejh.2023.3577

Publisher's note: all claims expressed in this article are solely those of the authors and do not necessarily represent those of their affiliated organizations, or those of the publisher, the editors and the reviewers. Any product that may be evaluated in this article or claim that may be made by its manufacturer is not guaranteed or endorsed by the publisher.